

## Synthesis, Photophysics and Photochemistry of Novel Luminescent Rhenium(I) Photoswitchable Materials

Vivian Wing-Wah Yam,\* Victor Chor-Yue Lau and Kung-Kai Cheung

Department of Chemistry, The University of Hong Kong, Pokfulam Road, Hong Kong

A series of new mono- and bi-nuclear rhenium(I) complexes,  $[\text{Re}(\text{CO})_3(\text{N}-\text{N})\text{L}]\text{ClO}_4$  and  $[\{\text{Re}(\text{CO})_3(\text{N}-\text{N})\}_2\text{L}'][\text{ClO}_4]_2$  [where  $\text{N}-\text{N} = 2,2'$ -bipyridine (bpy) or 1,10-phenanthroline (phen) and  $\text{L} = 4$ -phenylazopyridine (phazo), 4-styrylpyridine (stypy), 4-pyridyl-2-ethylbenzene (NB);  $\text{L}' = 4,4'$ -azopyridine (azo), 1,4-bis(4-pyridyl-2-ethyl)benzene (NBN)] are prepared and shown to exhibit rich photophysical and photochemical behaviour; the X-ray crystal structure of a binuclear  $[\{\text{Re}(\text{CO})_3(\text{bpy})\}_2(\text{NBN})][\text{PF}_6]_2$  complex is determined.

Recently, there has been growing interest in the design and development of photochemical molecular devices, in particular photoswitches.<sup>1</sup> Transition metal based molecular switches have been less well studied than their organic counterparts. The design of materials with nonlinear optical and/or liquid crystalline properties represents another growing area of research.<sup>2</sup> Transition metal based materials are especially attractive in that they have the additional advantage over their organic counterparts of offering a significant tunability on the structural and electronic properties of both the inorganic and organic components. Herein are described the synthesis, photophysics and photochemistry of a novel class of mono- and bi-nuclear rhenium(I) complexes; some of which have been shown to function as photoswitches by the incorporation of an azo moiety. The X-ray crystal structure of a binuclear rhenium(I) complex,  $[\{\text{Re}(\text{CO})_3(\text{bpy})\}_2(\text{NBN})][\text{PF}_6]_2$ , with a flexible bridging ligand, is also described.

$[\text{Re}(\text{CO})_3(\text{N}-\text{N})\text{L}]\text{ClO}_4$  and  $[\{\text{Re}(\text{CO})_3(\text{N}-\text{N})\}_2\text{L}'][\text{ClO}_4]_2$  [where  $\text{N}-\text{N} = 2,2'$ -bipyridine (bpy) or 1,10-phenanthroline (phen) and  $\text{L} = 4$ -phenylazopyridine (phazo), 4-styrylpyridine (stypy), 4-pyridyl-2-ethylbenzene (NB),  $\text{L}' = 4,4'$ -azopyridine (azo), 1,4-bis(4-pyridyl-2-ethyl)benzene (NBN)] were prepared by refluxing  $[\text{Re}(\text{CO})_3(\text{N}-\text{N})(\text{MeCN})\text{O}_3\text{SCF}_3$  (1 equiv.) and  $\text{L}$  (1.5 equiv.) or  $\text{L}'$  (0.5 equiv.) in dry THF under an inert atmosphere of nitrogen, respectively, following a procedure reported for related rhenium(I) complexes.<sup>3</sup> This was followed by subsequent recrystallization from acetonitrile–diethyl ether or dichloromethane–diethyl ether. All the newly synthesized complexes have been characterized by  $^1\text{H}$  NMR, positive-ion FAB-MS and gave satisfactory elemental analyses.† The X-ray crystal structure of  $[\{\text{Re}(\text{CO})_3(\text{bpy})\}_2(\text{NBN})][\text{PF}_6]_2$  has been determined.‡

The perspective drawing of the  $[\{\text{Re}(\text{CO})_3(\text{bpy})\}_2(\text{NBN})]^{2+}$  cation is depicted in Fig. 1. The coordination geometry at each Re atom is nearly octahedral with the three carbonyl ligands arranged in a facial fashion. At the Re centres, the *trans* angles subtended by  $\text{Re}^{\text{I}}$  and the two coordinated atoms *trans* to each other are in the range  $170(1)$ – $180(2)^\circ$ , showing a slight deviation from an ideal octahedral arrangement. The Re–C–O bond angles of  $168(3)$ – $177(3)^\circ$  are slightly distorted from linearity. The bond angles for  $\text{N}(1)$ – $\text{Re}(1)$ – $\text{N}(2)$  [ $75.0(8)^\circ$ ] and  $\text{N}(5)$ – $\text{Re}(2)$ – $\text{N}(6)$  [ $81(2)^\circ$ ] are much smaller than the  $90^\circ$  required by the bite distance exerted by the steric environment of the chelating bpy ligands. The  $\text{Re}(1)$ – $\text{C}(3)$  and  $\text{Re}(2)$ – $\text{C}(5)$  bond lengths of  $1.67(4)$  and  $1.74(4)$  Å, respectively, which are *trans* to the NBN ligand, are shorter than the other Re–C bonds. This is also consistent with the observation of the longer  $\text{C}(3)$ – $\text{O}(3)$  and  $\text{C}(5)$ – $\text{O}(5)$  bond distances. Similar observations have been reported for other related rhenium(I) systems.<sup>3g,4</sup>

The electronic absorption spectra of complexes **1**–**4**, **6** and **8** in dichloromethane and complexes **5** and **7** in acetonitrile at room temperature all show an absorption band at *ca.* 320–380 nm. With reference to previous spectroscopic work on rhenium(I) diimine systems,<sup>3</sup> this absorption band is tentatively assigned as the  $d_\pi(\text{Re}) \rightarrow \pi^*(\text{N}-\text{N})$  metal-to-ligand charge transfer (MLCT) transition. It is noteworthy that in the binuclear complexes **7** and **8**, the absorption coefficients for the MLCT

absorption band are about twice that observed for the respective mononuclear complexes **5** and **6**. Similar findings have been reported in other binuclear and supra-molecular systems.<sup>3g,5</sup> Excitation of the complexes at  $\lambda > 350$  nm in fluid solution at room temperature results in an intense yellowish green long-lived luminescence centred at *ca.* 500–580 nm. The photophysical data are summarized in Table 1. The large Stokes shift together with the long radiative lifetime of the excited state suggested that the origin of these emissions are of triplet parentage, possibly derived from the  $^3\text{MLCT}$  state. The photophysical data are comparable to those observed in the related  $[\text{Re}(\text{CO})_3(\text{bpy})(4\text{-Et-py})]\text{ClO}_4$  and  $[\text{Re}(\text{CO})_3(\text{phen-py})]\text{ClO}_4$  complexes.<sup>3</sup> The almost identical excited-state lifetimes and emission maxima of the binuclear complexes **7** and **8** with their respective mononuclear complexes **5** and **6** is

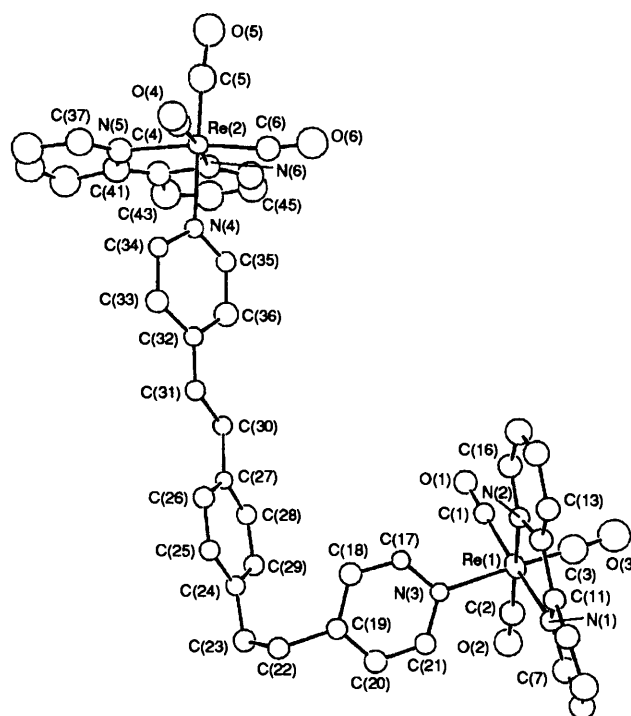


Fig. 1 Perspective drawing of the complex cation of **7** with atomic numbering scheme. Hydrogen atoms have been omitted for clarity. Thermal ellipsoids are shown at the 25% probability levels. Selected bond lengths (Å) and angles ( $^\circ$ ):  $\text{Re}(1)$ – $\text{C}(1)$  1.98(3),  $\text{Re}(1)$ – $\text{C}(2)$  1.79(4),  $\text{Re}(1)$ – $\text{C}(3)$  1.67(4),  $\text{Re}(1)$ – $\text{N}(1)$  2.24(2),  $\text{Re}(1)$ – $\text{N}(2)$  2.13(2),  $\text{Re}(1)$ – $\text{N}(3)$  2.18(2),  $\text{Re}(2)$ – $\text{C}(4)$  1.91(4),  $\text{Re}(2)$ – $\text{C}(5)$  1.74(4),  $\text{Re}(2)$ – $\text{C}(6)$  1.86(4),  $\text{Re}(2)$ – $\text{N}(4)$  2.19(2),  $\text{Re}(2)$ – $\text{N}(5)$  2.17(3),  $\text{Re}(2)$ – $\text{N}(6)$  2.24(3),  $\text{C}(1)$ – $\text{O}(1)$  1.14(3),  $\text{C}(2)$ – $\text{O}(2)$  1.23(4),  $\text{C}(3)$ – $\text{O}(3)$  1.26(5),  $\text{C}(4)$ – $\text{O}(4)$  1.10(4),  $\text{C}(5)$ – $\text{O}(5)$  1.27(5),  $\text{C}(6)$ – $\text{O}(6)$  1.18(5),  $\text{C}(22)$ – $\text{C}(23)$  1.55(5),  $\text{C}(30)$ – $\text{C}(31)$  1.50(4);  $\text{C}(1)$ – $\text{Re}(1)$ – $\text{N}(1)$   $171(2)$ ,  $\text{C}(2)$ – $\text{Re}(1)$ – $\text{N}(2)$   $172(1)$ ,  $\text{C}(3)$ – $\text{Re}(1)$ – $\text{N}(3)$   $179(2)$ ,  $\text{C}(4)$ – $\text{Re}(2)$ – $\text{N}(4)$   $173(1)$ ,  $\text{C}(5)$ – $\text{Re}(2)$ – $\text{N}(5)$   $180(2)$ ,  $\text{C}(6)$ – $\text{Re}(2)$ – $\text{N}(6)$   $170(1)$ ,  $\text{N}(1)$ – $\text{Re}(1)$ – $\text{N}(2)$   $75.0(8)$ ,  $\text{N}(5)$ – $\text{Re}(2)$ – $\text{N}(6)$   $81(2)$ ,  $\text{Re}(1)$ – $\text{C}(1)$ – $\text{O}(1)$   $174(3)$ ,  $\text{Re}(1)$ – $\text{C}(2)$ – $\text{O}(2)$   $177(3)$ ,  $\text{Re}(1)$ – $\text{C}(3)$ – $\text{O}(3)$   $176(4)$ ,  $\text{Re}(2)$ – $\text{C}(4)$ – $\text{O}(4)$   $169(3)$ ,  $\text{Re}(2)$ – $\text{C}(5)$ – $\text{O}(5)$   $175(4)$ ,  $\text{Re}(2)$ – $\text{C}(6)$ – $\text{O}(6)$   $168(3)$ .

Table 1 Photophysical data of the rhenium(I) complexes

Complex	Absorption <sup>a</sup> $\lambda_{\max}/\text{nm}(\epsilon/\text{dm}^3 \text{ mol}^{-1} \text{ cm}^{-1})$	Emission	
		Medium (T/K)	$\lambda_{\text{em}}/\text{nm} (\tau_0/\mu\text{s})$
1 $[\{\text{Re}(\text{CO})_3(\text{bpy})\}_2(\text{azo})][\text{ClO}_4]_2$	250 (10 085), 272 (9965), 321 (6535), 366 (4085)	$\text{CH}_2\text{Cl}_2$	535 (1.04 $\pm$ 0.10)
2 $[\text{Re}(\text{CO})_3(\text{bpy})(\text{phazo})]\text{ClO}_4$	300sh (25 425), 315 (40 000), 321sh (9400), 344 (36 350)	$\text{CH}_2\text{Cl}_2$	550 (0.50 $\pm$ 0.05)
3 $[\text{Re}(\text{CO})_3(\text{phen})(\text{phazo})]\text{ClO}_4$	232 (16 130), 260 (11 000), 279 (12 950), 300 (9400), 343 (11 770), 450sh (5000)	$\text{CH}_2\text{Cl}_2$	563 (0.2, 1.5 $\pm$ 0.1) <sup>b</sup>
4 $[\text{Re}(\text{CO})_3(\text{phen})(\text{stypy})]\text{ClO}_4$	276 (24 200), 338 (24 500), 400sh (2915)	$\text{CH}_2\text{Cl}_2$	548 (2.3 $\pm$ 0.2)
5 $[\text{Re}(\text{CO})_3(\text{bpy})(\text{NB})]\text{ClO}_4$	249 (19 150), 263 (18 870), 305 (11 225), 319 (11 980), 348 (3525)	MeCN <sup>c</sup> Solid (298) Solid (77)	540 (0.23 $\pm$ 0.02) 510 (1.5 $\pm$ 0.1) 500
6 $[\text{Re}(\text{CO})_3(\text{phen})(\text{NB})]\text{ClO}_4$	259 (27 500), 276 (29 985), 294sh (16 250), 334sh (5335), 368sh (4305)	$\text{CH}_2\text{Cl}_2$ MeCN Solid (298) Solid (77)	550 (2.0 $\pm$ 0.2) 571 (1.4 $\pm$ 0.1) 515 (1.9 $\pm$ 0.2) 500
7 $[\{\text{Re}(\text{CO})_3(\text{bpy})\}_2(\text{NBN})][\text{ClO}_4]_2$	249 (38 280), 263 (37 445), 305 (21 700), 319 (22 870), 347 (6710)	MeCN Solid (298) Solid (77)	586 (0.20 $\pm$ 0.02) 508 (1.2 $\pm$ 0.1) 508
8 $[\{\text{Re}(\text{CO})_3(\text{phen})\}_2(\text{NBN})][\text{ClO}_4]_2$	259 (43 205), 275 (47 650), 295sh (24 560), 329sh (8490), 383sh (5825)	$\text{CH}_2\text{Cl}_2$ MeCN Solid (298) Solid (77)	550 (2.5 $\pm$ 0.2) 570 (1.5 $\pm$ 0.1) 557 (1.1 $\pm$ 0.1) 540

<sup>a</sup> All absorption spectra are recorded using  $\text{CH}_2\text{Cl}_2$  as solvent, except complexes 5 and 7, using MeCN as solvent. <sup>b</sup> A biexponential decay. <sup>c</sup> Not recorded in  $\text{CH}_2\text{Cl}_2$  as solubility in  $\text{CH}_2\text{Cl}_2$  is too low.

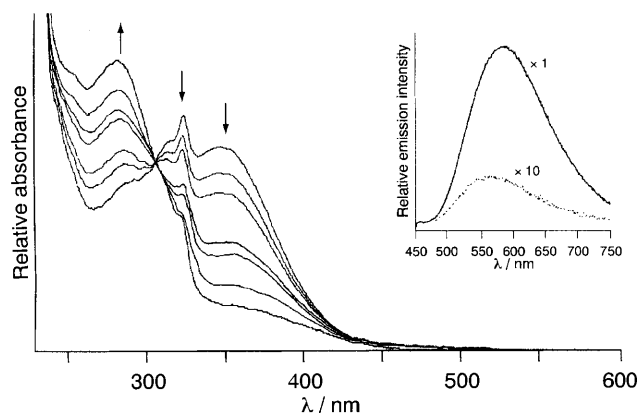


Fig. 2 The UV-VIS spectral trace of complex 2 upon steady-state photolysis at  $\lambda > 350$  nm at 0, 125, 190, 250, 370, 490, 790 min. The insert shows the emission spectra before (---) and after (—) the photolysis.

suggestive of independent non-interacting rhenium centres, typical of complexes containing nonconjugated bridging ligands.<sup>3g</sup>

With complexes 1–3, where L or L' contains a photo-isomerizable azo moiety, visible-light excitation induces a photochemical change. Irradiation of a degassed dichloromethane solution of  $[\text{Re}(\text{CO})_3(\text{bpy})(\text{phazo})]\text{ClO}_4$  2 at  $\lambda > 350$  nm produced spectral changes as shown by a clean UV-VIS spectral trace with an isosbestic point observable at ca. 310 nm (Fig. 2). It is likely that these spectral changes are associated with the *trans*-*cis* isomerization of the azo moiety. To our surprise, the emission intensity was shown to be greatly enhanced after steady-state photolysis for 13 h. For complex 2, the luminescence quantum yield ( $\phi_{\text{lum}}$ ) measured after photolysis is ca. 40 times greater than that before photolysis, and its emission maximum is red-shifted by ca. 20 nm. Similar findings

have been obtained for both complexes 1 and 3. It is well known that for the free azo chromophore, the triplet state energy for the *trans*-isomer is generally lower than the *cis*-counterpart.<sup>6</sup> Thus it is likely that in the <sup>3</sup>MLCT excited state, some of its excited state energy is intramolecularly transferred to the *trans*-azo moiety, providing an additional non-radiative deactivation pathway. On the other hand, with the *cis*-azo ligand formed upon photolysis, such intramolecular energy transfer processes are highly disfavoured or blocked owing to the higher triplet state energy of the *cis*-isomer,<sup>6</sup> resulting in a higher luminescence quantum yield (for complex 2,  $\phi_{\text{lum}}(\text{trans}) = 0.027$ ;  $\phi_{\text{lum}}(\text{cis}) = 7.2 \times 10^{-4}$  according to the method of Demas and Crosby).<sup>7</sup> The insert in Fig. 2 shows the relative emission intensity of complex 2 before and after photolysis. In order to further our understanding on the photoinduced *trans*-*cis* isomerization processes in these complexes, a comparison of their photoreactivities with the bridging C=C analogues of complexes 1–3 was made. As expected, due to the relatively higher triplet state energy of the ethylene moiety<sup>6</sup> compared to the azo analogue, the steady-state photolysis reaction of complex 4 was found to be extremely slow under similar experimental conditions. Exhaustive mechanistic investigations on the photochemical reactivity of these luminescent materials and on the identity of the photolysed products are in progress.

V. W. W. Y. acknowledges financial support from the Research Grants Council and The University of Hong Kong. V. C.-Y. L. acknowledges the receipt of a Croucher studentship administered by the Croucher Foundation.

Received, 24th October 1994; Com. 4/064871

#### Footnotes

† 1: <sup>1</sup>H NMR [270 MHz,  $(\text{CD}_3)_2\text{CO}$ , 298 K, relative to  $\text{SiMe}_4$ ]:  $\delta$  8.0–9.0 (m, 16H, bpy H), 7.8, 9.5 (dd, 8H, pyridyl H). Positive FAB-MS: ion clusters at  $m/z$  1138  $\{\text{M} + \text{ClO}_4\}^+$ , 1039  $\{\text{M}\}^+$ . 2: <sup>1</sup>H NMR:  $\delta$

8.0–8.9 (m, 8H, bpy H), 7.8, 9.5 (dd, 4H, pyridyl H), 7.4–7.6, 7.9–8.0 (m, 5H, phenyl H). Positive FAB-MS:  $m/z$  610  $\{M\}^+$ , 427  $\{M - \text{phazo}\}^+$ . **3:**  $^1\text{H NMR}$ :  $\delta$  8.3–8.9, 10.0 (m, 8H, phen H), 7.8, 9.1 (dd, 4H, pyridyl H), 7.4–7.7 (m, 5H, phenyl H). Positive FAB-MS:  $m/z$  634  $\{M\}^+$ , 451  $\{M - \text{phazo}\}^+$ . **4:**  $^1\text{H NMR}$ :  $\delta$  7.0, 7.4 (d, 2H, vinyl H), 7.3–7.5 (m, 5H, phenyl H), 8.0–8.8 (m, 8H, phen H), 7.2, 9.6 (dd, 4H, pyridyl H). Positive FAB-MS:  $m/z$  632  $\{M\}^+$ , 451  $\{M - \text{stypy}\}^+$ . **5:**  $^1\text{H NMR}$ :  $\delta$  2.8–2.9 (m, 4H,  $-\text{CH}_2\text{CH}_2-$ ), 7.0–7.3 (m, 7H, phenyl H and pyridyl H *meta* to N), 8.4 (d, 2H, pyridyl H *ortho* to N), 7.7–8.3, 9.2 (m, 8H, bpy H). Positive FAB-MS:  $m/z$  610  $\{M\}^+$ , 427  $\{M - \text{NB}\}^+$ . **6:**  $^1\text{H NMR}$ :  $\delta$  2.6–2.9 (m, 4H,  $-\text{CH}_2\text{CH}_2-$ ), 6.9–7.2 (m, 7H, phenyl H and pyridyl H *meta* to N), 8.0–9.5 (m, 10H, phen H and pyridyl H *ortho* to N). Positive FAB-MS:  $m/z$  634  $\{M\}^+$ , 451  $\{M - \text{NB}\}^+$ . **7:**  $^1\text{H NMR}$ :  $\delta$  2.7–2.9 (m, 8H,  $-\text{CH}_2\text{CH}_2-$ ), 6.8 (s, 4H, phenyl H), 7.0–9.2 (m, 24H, pyridyl and bpy H). Positive FAB-MS:  $m/z$  1138  $\{M\}^+$ . **8:**  $^1\text{H NMR}$ :  $\delta$  2.5–2.8 (m, 8H,  $-\text{CH}_2\text{CH}_2-$ ), 6.8 (s, 4H, phenyl H), 7.0–9.6 (m, 24H, pyridyl and phen H). Positive FAB-MS:  $m/z$  1287  $\{M + \text{ClO}_4\}^+$ , 1188  $\{M\}^+$ .

‡ *Crystal data for 7:*  $\text{C}_{46}\text{H}_{36}\text{F}_{12}\text{N}_6\text{O}_6\text{P}_2\text{Re}_2$ ;  $M_f = 1431.17$ ; monoclinic, space group  $P2_1/c$ , crystal dimensions  $0.05 \times 0.05 \times 0.40$  mm,  $a = 8.515(2)$ ,  $b = 22.032(4)$ ,  $c = 26.703(3)$  Å,  $\beta = 92.04(1)^\circ$ ,  $V = 5006.4(1.0)$  Å<sup>3</sup>,  $Z = 4$ ,  $D_c = 1.899$  g cm<sup>-3</sup>,  $\mu(\text{Mo-K}\alpha) = 50.56$  cm<sup>-1</sup>,  $F(000) = 2760$ ,  $T = 297$  K, no. of parameters = 317,  $R = 0.066$  and  $R_w = 0.075$  for 2697 observed data with  $I \geq 3\sigma(I)$  ( $w = 4 F_o^2/\sigma^2(F_o^2)$ , where  $\sigma^2(F_o^2) = [\sigma^2(I) + (0.060 F_o^2)^2]$ ). Diffraction data were collected on an Enraf-Nonius CAD-4 diffractometer with graphite monochromated Mo-K $\alpha$  radiation ( $\lambda = 0.71073$  Å). The structure was solved by Patterson and Fourier methods and subsequent refinement by full-matrix least squares using the Enraf-Nonius SDP-1985 Programs (Enraf-Nonius Structure Determination Package, SDP, Enraf-Nonius, Delft, 1985) on a MicroVAX II computer. Atomic coordinates, bond lengths and angles, and thermal parameters have been deposited at the Cambridge Crystallographic Data Centre. See Information for Authors, Issue No. 1.

## References

- 1 V. Balzani and F. Scandola, *Supramolecular Photochemistry*, Ellis Horwood, Chichester, 1991; F. Vögtle, *Supramolecular Chemistry*, Wiley, Chichester, 1993.
- 2 *Materials for Nonlinear Optics, Chemical Perspectives*, ed. S. R. Marder, J. E. Sohn and G. D. Stucky, *ACS Symp. Ser.*, 1991, **455**; *Inorganic Materials*, ed. D. W. Bruce and D. O'Hare, Wiley, Chichester, 1992; D. W. Bruce and X.-H. Liu, *J. Chem. Soc., Chem. Commun.*, 1994, 729; F. Barigelletti, L. Flamigni, V. Balzani, J.-P. Collin, J.-P. Sauvage, A. Sour, E. C. Constable and A. M. W. Cargill-Thompson, *J. Chem. Soc., Chem. Commun.*, 1993, 942; G. Jia, R. J. Puddephatt, J. J. Vittal and N. C. Payne, *Organometallics*, 1993, **12**, 263.
- 3 (a) M. S. Wrighton and D. L. Morse, *J. Am. Chem. Soc.*, 1974, **96**, 998; (b) M. S. Wrighton, D. L. Morse and L. Pdungsap, *J. Am. Chem. Soc.*, 1975, **97**, 2073; (c) S. M. Fredericks, J. C. Luong and M. S. Wrighton, *J. Am. Chem. Soc.*, 1979, **101**, 7415; (d) J. V. Caspar and T. J. Meyer, *J. Phys. Chem.*, 1983, **87**, 952; (e) G. Tapolsky, R. Duesing and T. J. Meyer, *Inorg. Chem.*, 1990, **29**, 2285; (f) J. R. Shaw and R. H. Schmehl, *J. Am. Chem. Soc.*, 1991, **113**, 389; (g) R. Lin, Y. Fu, C. P. Brock and T. F. Guarr, *Inorg. Chem.*, 1992, **31**, 4346.
- 4 E. Horn and M. R. Snow, *Aust. J. Chem.*, 1980, **33**, 2369; P. Chen, M. Curry and T. J. Meyer, *Inorg. Chem.*, 1989, **28**, 2271; S. A. Moya, J. Guerrero, R. Pastene, R. Schmidt, R. Sariego, R. Sartori, J. Sanz-Aparicio, I. Fonseca and M. Martinez-Ripoll, *Inorg. Chem.*, 1994, **33**, 2341.
- 5 See, for example, G. Denti, S. Campagna, L. Sabatino, S. Serroni, M. Ciano and V. Balzani, *Inorg. Chem.*, 1990, **29**, 4750.
- 6 S. L. Murov, *Handbook of Photochemistry*, Marcel Dekker, New York, 1973; D. G. Whitten and M. T. McCall, *J. Am. Chem. Soc.*, 1969, **91**, 5097.
- 7 J. N. Demas and G. A. Crosby, *J. Phys. Chem.*, 1971, **75**, 991.